BVS 2203
REV
DATE 29 June 1987

ORIGINATORS R.W. Lieske

D.L. Ometz

OLS L CHANNEL GAIN CORRECTION

FOR NON-LAMBERTIAN SCENES

Contract F04701-86-C-0078

Prepared For

UNITED STATES AIR FORCE
Headquarters, Space Division
Los Angeles, California

Prepared By

WESTINGHOUSE ELECTRIC CORPORATION
Defense and Electronics Center
Baltimore, Maryland

BVS No. 2203

REVISION SHEET & NOTES PAGE

REVISION LETTER	REVISION DATE	AFFECTED PAGES	REVISION MADE BY
-	06/21/87	All pages.	LIESKE

(* INDICATES PAGE # IS ONLY CHANGE TO THAT PAGE)

Notes:

WANG Doc. #(s): e/0401B

Table of Contents

OLS L Channel Gain Control for Non-Lambertian Scenes

Abstract

Scene anisotropy is not compensated for in the present Block 5D-2 OLS systems and therefore scene data saturation occurs. The worst case deviation from Lambertian scene characteristics is 15.6db (600 percent) and occurs for illumination source angles greater than 60 degrees due to the forward scatter specular component.

The OLS L channel (0.4-1.0 um) gain control software has been modified to prevent non-Lambertian scenes from saturating the data. A reference scene Bidirectional Reflectance Distribution Function (BRDF) is used to determine the gain reduction or increase necessary based on knowledge of the relative positions of the spacecraft, illumination source, and scene. The reference BRDF selected for earth scenes is modeled upon empirical data from the Nimbus-7 Earth Radiation Budget (ERB) experiment. The ocean surface has the greatest anisotropy, and was therefore selected as the base for modeling the reference BRDF. Lower anisotropic scenes will yield reduced output but are expected to provide reasonable imagery. Scene data could be reprocessed with knowledge of scene type to restore optimum response. This is only possible since the information is still present in the unsaturated data. The OLS flight software containing the modified gain control algorithm can be uploaded and implemented in on-orbit OLS systems.

1.0 Introduction

At present the OLS L channel gain is controlled as a function of the scene solar elevation (SSE), presuming that scene variations from Lambertian characteristics are part of the desired data. The actual scene BRDF results in glint due to solar reflections in near noon orbit, and in forward scatter saturations at the edge of scan in terminator orbits. Similar effects occur when the moon is the source of scene illumination and is appropriately positioned. These phenomena interfere with the desired data from the scene. As a result, a gain control algorithm has been developed that compensates for the anisotropy of a reference scene to prevent these data saturations. It is implementable in on-orbit OLS systems, once the Revision K OLS software is uploaded.

2.0 Basic Approach

Gain control of the OLS L channel in the along scan gain control (ASGC) mode has previously used knowledge of incident scene illumination to establish radiant exitance of a 0.8 albedo Lambertian scene as the full scale output. Non-Lambertian scene radiant exitance can exceed full scale if the albedo and increased directional reflectance combine with sufficient magnitude. Once saturation occurs all information concerning differential scene characteristics becomes masked and is unrecoverable. By choosing the most anisotropic scene BRDF as a reference BRDF, and using it to control sensor gain, saturation due to non-Lambertian scenes is prevented. In effect, the established full scale output becomes the radiant exitance from a 0.8 albedo scene having the reference BRDF.

While this approach prevents the receipt of saturated data due to non-Lambertian scenes, it also reduces to output from scenes which have less anisotropy than the reference BRDF. It is anticipated that some users will reprocess the data with a knowledge of the scene type (and therefore scene reflectance pattern) so as to restore optimum response. However, immediate imagery usage is expected to benefit even in the absence of reprocessing. Certainly the lack of saturation will present more usable data for scenes whose reflectance pattern is close to the

reference BRDF such as clouds and water. Even those scenes whose BRDF is more isotropic than the reference BRDF such as land should be quite usable since they will appear darkened. Contrast with clouds will be maintained and automatic data processing using a threshold will continue to be feasible.

A mathematical model representing the reference scene BRDF was developed as the basis of L channel gain control. Theoretical and empirical BRDF studies were researched to determine an optimal reference BRDF. The reference chosen was derived from Nimbus-7 over-ocean scene imagery. This empirical pattern has been smoothed and made symmetrical to facilitate modeling. Based on this data, an algorithm was formulated which defines a gain correction factor to be applied to the L-channel for all scene, illumination source (sun or moon) and spacecraft relative positions. The correction factor is used to change the DLS gain values to compensate for the anisotropy of both sunlit and moonlit scenes.

3.0 Describing Scene Reflectance

3.1 Nomenclature of Scene Reflectance

Albedo - The total radiant reflectance for a particular incident beam geometry; the fraction of the total light incident on a reflecting surface which is reflected in all directions for a particular incident beam geometry.

Bidirectional Reflectance Distribution Function (BRDF) - a derivative, a distribution function, relating the irradiance incident from one given direction to its contribution to the reflected radiance in another direction.[3] A unified notation for the specification of reflectance in terms of both incident- and reflected-beam geometry introduced by Nicodemus et al[2];

Lambertian Scene - a scene for which radiance is constant for all view angles in the hemisphere of reflection; a scene which appears equally bright in all directions regardless of how it is irradiated[3]; Synonyms: isotropic scene, perfectly diffuse scene; Antonyms: anisotropic scene, specular scene.

Anisotropic Reflectance Factor - The ratio of the reflected radiance from an anisotropic scene at a particular geometry of incident and reflected beams, to the reflected radiance of an isotropic scene with the same albedo.

Reflectance Pattern - The scene reflected radiance pattern that is comprised of the anisotropic reflectance factors for all reflected beam geometries at a particular incident beam geometry; scene BRDF at a particular incident beam geometry normalized to the albedo of the scene.

BRDF Normalized (BRDFN) - The set of reflectance patterns representing all incident beam geometry; scene BRDF normalized to scene albedo.

3.2 Geometry of Scene Reflectance

Figure 1 shows the reflectance geometry and angular nomenclature as used by Taylor and Stowe to present reflectance data from the Nimbus-7 ERB.[1] Knowledge of the incident, reflected, and azimuthal angle is necessary and sufficient to describe the scene BRDFN. To facilitate implementation of the BRDF gain correction algorithm in the OLS, it was necessary to characterize BRDFN as a function of the available spacecraft data: the cosine of the solar azimuth, solar elevation and OLS scan angle. Figure 2a,b, and c defines these angles.

The BRDFN is characterized by Taylor and Stowe as a set of reflectance patterns. Each reflectance patterns. Each reflectance pattern has a set of isopleths (contour lines) of the constant anisotropic reflectance factors. (See Figures 3a thru 3f) In the reflectance patterns, isopleths with a value of one indicate radiance from scenes equal to radiance from an isotropic (Lambertian) scene. Values greater than one indicate that scene radiance is greater than radiance from an isotropic scene. Scenes with reflectance factors different than one indicate that the scene is exhibiting non-Lambertian characteristics. All natural earth scenes exhibit some anisotropy.

3.3 Earth Scene Reflectance

Significant variations in the magnitude of the anisotropic reflectance factors are found for different earth scene types (e.g. land, snow, clouds, and ocean). The ocean scene was found to have the most anisotropy (i.e. largest variations in reflectance factor). High clouds, mid clouds, and low clouds follow in order of decreasing magnitude. Snow, although having a high albedo, has small variation in its anisotropic reflectance factor. Land, in general, was found to be among the least anisotropic. The pattern for water which was selected as reference, contains both specular and diffuse characteristics. Of the two, the specular component is dominant. It is characterized by large variations in reflectance in the principle plane of the illuminating source. The viewing angle at which the specular component is maximum is equal to the angle of incidence for low source angles, as predicted by the law of reflection for a specular surface. Theoretical analysis and experimentation[16,17] predicts an off-specular maxima in the BRDFN which emerges as the source angle increases for "rough" surfaces. Empirical data also indicates, for larger source angles, an off-specular maxima which increases with source angle, and is attributed to surface roughness (e.g. sea state in the ocean). The diffuse component of the BRDFN has little azimuthal variation and makes only a small contribution to the scene anisotropy. The diffuse component accounts for increased backscatter.

4.0 Reference BRDF Data Base

4.1 Selection

Empirical data from the Nimbus-7 ERB experiment was selected, since this was the only data base found to contain a large sampling of information in the visible spectral range on the anisotropy of all types of uniform earth scenes: land, ocean, snow, and four cloud types. The data from the Nimbus-7 ERB experiment was collected over a 61 day period during 1978 using a radiometer (0.2-4.5 um). Previous experiments - such as the TIROS[6], NASA Convair[7,8], and other plane and

balloon flights[10,11] had limited samplings of data and scene type. Theoretical scattering models have been developed[12,13,14,15] but they are limited to single scene types and the calculations in many instances are not suitable for OLS implementation. The angular patterns of these other investigations, however, are in qualitative agreement with those found in the Nimbus-7 ERB experiment for the different scene types.

4.2 Limitations

The Nimbus-7 data selected for the development of a reference scene BRDF model had one drawback. The sensitivity range of the Nimbus radiometer was in the broadband visible range of 0.2-4.5 um, whereas the OLS L-channel HRD detector sensitivity is in the narrower visible 0.4-1.0 um range. Although the sensitivity ranges differ, a scaling factor was estimated based on a study[8] comparing the average reflectance values obtained from a 0.2-4.0 um. band to one with a 0.55-0.85 um window. The study was based on a few limited cases in the principal plane of the sun. A scaling factor based on this limited data has been incorporated into the specular component of the BRDF model.

5.0 Reference BRDF Modeling

The BRDFN for water from the Nimbus-7 ERB experiment radiometer is represented by Taylor and Stowe on a polar coordinate grid for various sun angle ranges in Figures 3-a thru 3-f. To facilitate modeling, data was smoothed as shown in Figures 4-a thru 4-f. The data was plotted on a rectilinear coordinate system and further smoothed as shown in Figures 5-a thru 5-f.

The variation of the contour values in dB with each parameter was determined by holding constant two of three angular parameters (solar zenith angle(δ), satellite zenith angle (θ), and azimuth (α)) and determining the variation in gain versus the third angular parameter. The equations were then converted to dependance on the available spacecraft data: cosine solar azimuth, solar elevation and scan angle. Lunar parameters replace solar when the moon is the source. This enabled formulation of the algorithm to characterize the gain control shown in Figure 8.

5.1 Equations Describing BRDF Correction

Equation 1 derives the azimuth angle (α) from the cosine of the azimuth (cos(AZ) which is provided to the OLS. Equation 2 derives the scale factor (K5) for use in the diffuse components computation (Eq. 5). Equation 3 derives the scene source elevation (γ) based on the source elevation (El), at nadir geocentric scan angle (θ) and the cosine of the azimuth (cos(Az)). Equation 4 derives the OLS view angle (sensor zenith angle) of the scene (θ) from sensor centric scan angle (ϕ) and geocentric scan angles (θ).

Equation 5 is the expression for the diffuse BRDF correction (in decibels) as a function of the scene source elevation (γ), OLS view angle of the scene (θ) and the source Azimuth (Az) via the K5 term.

Equations 6a thru 6c approximate the angle of the specularly reflected beam measured from the scene zenith (S^1). Equation 7 approximates the angle between specularly reflected beam and the OLS view angle to the scene (θ^1). It is a law of cosines approximation for the exact expression in spherical coordinates necessary to save processor time in the OLS. Eq. 8 determines the angular extent of the region where specular BRDF correction is to be made. The angular extent ($\Delta\ \theta$) and thus ground scene affected by the specular BRDF correction is a function of the scene solar elevation (γ). Eq. 9 computes the scaled deviation between the OLS view angle of the scene and the specularly reflected beam (X). This quantity will be used in Eq. 11 to control the amount of specular BRDF correction applied based on the closeness of the OLS line-of-sight to the specularly reflected beam. An adjustable scale factor (BRDFX2) has been applied to this expression. The peak value of specular BRDF correction (MAXSPEC) based on the scene source elevation. A sensitivity correction factor has been applied to allow for the greater sensitivity of the OLS detectors to BRDF effects as compared to the Nimbus-7 radiometer. Eq. 11 derives the amount of gain reduction (RS) to compensate for the specular BRDF component. The specular component is scaled down parabolically as a function of the square of the angle away from the

maximum specular direction. An adjustable scale factor has been applied to correct for any sensitivity different between the HRD (L-day) and PMT (L-night) detectors in the OLS since they have different spectral responses.

Eq. 12 clamps the specular component to zero for values of $X^2_{\geq}$ indicating that the OLS line-of-sight is adequately displaced from the specularly reflected beam to avoid the need for specular BRDF gain reduction. Eq. 13 combines the diffuse and specular components of the BRDF gain correction algorithm to provide one gain correction (R dB) to be applied in the OLS Along Scan Gain Control.

5.2 Pattern of Numerical BRDF Model

Plots illustrating the mathematical model of the BRDF are in Figures 6 and 7. Figure 7 contains the scaling factor to correct for the differing channel response wavelength ranges between the Nimbus-7 radiometer and the OLS. The plots were generated with a personal computer with graphics capability. Note that the anisotropic reflectance factors in these plots are in units of gain (db.) to facilitate OLS implementation. For comparison purposes, the gain ratio representing the anisotropic reflectance factor as used in the empirical plots is listed along with the gain value.

5.3 Model Deviations

The maximum deviation arising in the pattern between the numerical BRDF model and the empirical BRDF pattern appears to be on the order of 2 db in the region of the specular component where BRDF correction gain values change at a rate of 1 db. per 5 degrees source elevation. The maximum deviation appears for values of high source elevation and in the range of azimuth, elevation, and scan angles where the specular component is dominant.

$$\alpha = 90° - \sin^{-1}(\cos(Az)) \quad (1)$$

$$K5 = (1 - 0.375 \sin(V))/90° \quad (2)$$

For each geocentric scan angle θ

$$\gamma = El + \theta * \cos(Az) \quad (3)$$

$$\theta = \theta + \phi \text{ Diffuse component} - RV, \quad (4)$$

$$RV = (-5.77 + +0.559\ \gamma) + (13.77 - 0.1242\ \phi) * K5 * \theta \quad (5)$$

Piecewise approximation to the specular reflection angle - δ'

$$\delta' = 90° \quad (6a)$$

$$\text{If } \phi > 30°,\ \delta' = 150° - 2\gamma \quad (6b)$$

$$\text{If } \phi > 60°,\ \delta' = 90° - \phi \quad (6c)$$

Approximation for angle from the reflected maxima centroid,

$$(\theta'^2) = (\delta')^2 + (\theta)^2 - 2 * \theta * SGN(\theta) * \cos(Az) * \delta' \quad (7)$$

$$\Delta\theta = 17 + 9 \sin(4\gamma + 50°) = \text{Radius of circular disc} \quad (8)$$

$$x^2 = (\theta'^2) * 0.106/(\Delta\theta)^2 \quad \text{Deviation from Specular Max} \quad (9)$$

↑

BRDFX2 constant

Specular Peak Value $MAXSPEC = 9.3 + 4 \sin(4\gamma + 50°)$ (10)

↑

(7.5 + sensitivity correction of 1.8dB)

Final specular calculation $RS = SENKP * MAXSPEC * (1 - x^2)$ (11)

↑

PMT/HRD scale factor

$RS = 0$ for $(1 - x^2) < 0$ (e.g. no specular component) (12)

Summation of Diffuse and Specular components (13)

A positive value indicates a required decrease in system gain.

$R = RV + RS$ (db).

Figure 8 - BRDF Model Equations

Table ___. BRDF Variables

RV = diffusely backscattered component, dB

RS = specularly reflected component, dB

R = amount that OLS gain should be reduced to compensate for increased BRDF of scene (reduce gain for positive R), dB

= RV + RS

S = illumination source elevation angle on scene (see Figure 1)

S' = specularly reflected ray deviation angle measured from the scene normal

α = illumination source azimuth angle on scene. (See Figure 1)

θ = OLS view angle, wrt scene normal; sensor zenith of scene angle

AZ = angle between the projection of the spacecraft/sun (or moon) line upon the y-z plane where the y direction is along track and the z direction is along scan perpendicular to the s/c track direction. A positive azimuth corresponds to a spacecraft/sun line with a positive component along the +y axis. The ty direction is the normal direction of s/c travel.

EL = the elevation (solar or lunar) is the angle between the spacecraft sun line and the y-z plane where the y-direction is along track and the z direction is along scan perpendicular to the s/c track direction. The +z axis is directed forward nadir. A positive solar elevation corresponds to a spacecraft sun line with a negative component along the +x axis.

Table ___. BRDF Variables (continued)

γ = scene illumination source elevation; angle between satellite +z axis and sun line.

= EL + θ * cos(AZ)

K5 = scale factor utilized in the diffuse component based on azimuth

θ = OLS sensor centric scan angle

θ = OLS geocentric scan angle

θ' = angle between the specularly reflected ray and the OLS line-of-sight

WR = angular extent of the specular BRDF correction

X = scale factor quantifying the deviation between the OLS line-of-sight and the specularly reflected maxima

MAXSPEC = peak amount of specular gain correction possible as a function of the scene solar elevation (γ)

BRDFX2 = adjustable scale factor affecting the angular extent of the specular BRDF correction

SENKP = adjustable scale factor used to correct for differences between HRD and PMT detector sensitivities to specular BRDF effects. It also scales the magnitude of specular BRDF correction

6.0 OLS Implementation

6.1 Simplified Gain Control Algorithm

Gain control of the OLS L channel is accomplished by a combination of hardware and software. The hardware implements dynamic gain control using a software initialized value at the beginning of scan that is incremented at a linear rate versus time. The software provides updated inputs to vary the rate of gain change versus time approximately every 4ms of scan so as to approximate the ideal gain function over the scan with about 18 linear segments. The desired rate of gain change is determined by subtracting desired gain at the next update and the actual gain at the current update and then dividing by the time between the updates. In order to stay within the time constraints of the OLS processor and incorporate scene BRDF gain control, the algorithm for determining the desired gain at the next update was simplified.

6.1.1 Previous Gain Control Algorithm

The previous method of determining the desired gain computed the scene solar elevation at the next update and then performed a table lookup with interpolation from the Gain Value Versus Scene Solar Elevation (GVVSSE) table to determine the desired gain.

6.1.2 New Gain Control Algorithm

The new method of determining the desired gain computes the scene geocentric scan angle at the next update and then obtains the desired gain from a table lookup with interpolation from the Gain Function table. The Gain Function table contains gain value versus scene geocentric scan angle. During each overscan one of the 31 entries in the Gain Function table is computed so that 2.6 sec is required to fully update the table.

6.2 Gain Function Algorithm

The equations of Figure 8 defining the BRDF gain correction are incorporated in an algorithm for OLS implementation. The OLS uses the end of scan time to perform the BRDF and other gain calculations and puts the desired gain as a function of geocentric scan angle into the Gain Function table The gain along scan will be found by interpolating between gain values in this table. Normally, one value in the Gain Function table will be updated at each end of scan. Only in instances where a processor load occurs will the required BRDF calculation during the end of scan period have to be skipped. The gain value in the table will be derived based on a knowledge of the relative moon, sun, spacecraft, and scene positions.

Location data for the sun and moon relative to the spacecraft is obtained from the spacecraft generated ephemeris. The gain from the solar GVVSSE curve, plus a solar BRDF gain correction value will be calculated along with a similar gain calculation for the lunar case. The corresponding radiance contributions from each is summed and converted to a gain value for the given scan angle which is entered in the gain table. An uplinkable constant in the specular component of the BRDF equations exists to compensate for any differences in the BRDF sensitivity of the HRD and PMT channels in the OLS due to slightly different channel wavelength bands. Some other constants in the BRDF equations are uplinkable for on-orbit tailoring.

The BRDF gain control algorithm may be applied over the entire range of scene solar elevation of -90 to +90 degrees, and to all possible azimuth and elevation angles as the spacecraft orbits the earth. OLS commands also permit use of specular component (RS) only, diffuse component only (RV), or no BRDF gain control at all. The reference BRDF was established with sunlight as the primary source of illumination, however, the BRDF gain correction algorithm will also apply with moonlight as the source in nightime scenes. For scattered and refracted sunlight just on the dark side of the terminator, the BRDF algorithm is unmodified except that it assumes the source illumination is at a sun angle of 85 degrees. For moonlit scenes, the lunar parameters will replace the solar parameters in the BRDF equations.

7.0 On-Orbit Verification Plans

The algorithm for BRDF gain correction will be implemented on orbit. Adjustments to the BRDF constants can and most likely will be necessary, to adjust the amount of BRDF gain correction to best fit the expected scene anisotropy.

8.0 Conclusion

Some saturations in the OLS data are a result of the anisotropic nature of the reflectance of some earth scenes. This can be remedied by implementing the BRDF gain correction algorithm in the OLSP software. The model is applicable for both sunlit and moonlit scenes. Terminator scenes whose primary illumination is reflected and refracted sunlight exhibit characteristics similar to scenes illuminated by positive low solar elevations, and are modeled as such.

Saturations of the data in the OLS system are as predicted by the BRDF of the scenes that have been determined empirically in the Nimbus-7 experiment. The greatest saturation in the OLS data has been in the terminator orbits at the edges of scan where the sun angle is large and the satellite is scanning in the principal plane of the sun. The greatest amount of anisotropic reflectance is predicted and occurs under these conditions. Poor scene return data also occurs in noon orbits when the sun (or moon) is near the scene normal (e.g. small source angle).

The elimination of glint by the BRDF correction algorithm will directly benefit the AWS global cloud cover analysis. Solar and lunar glint is predicted and does occur for the specular reflections from the earth scene. Current automated techniques to estimate cloud cover suppress processing of visible data over a rather large region of glint where δ and Θ are within 15° on the sunny side. The BRDF correction algorithm will allow this area to be used by lowering the gain by an amount based on the ocean reference BRDF to make the scene less than or equally bright than it would appear if it were isotropic.

The basic benefit of being able to use more visible data in automatic processing may have impacts on other users. For instance, use of sunglint patterns to determine sea state[19] may require revised methods of hardcopy inspection and perhaps removal of the OLS-applied gain correction during their ground processing of the data to restore the "uncorrected" scene data. An advantage of the OLS gain correction being applied is that it will enable retrieval of gray scale values for scene data which are currently fully saturated. In addition, the correction will eliminate data processing problems caused by glint and may enhance ability to determine the scene type.

An adcitional benefit of BRDF gain correction results from the diffuse component correction. The visible data has what is known as a look angle bias caused by the increased pathlength in the atmosphere and the aspect of clouds viewed as a function of sensor viewing angle (θ)[20]. This should be eliminated by the diffuse correction of BRDF gain control. The scene, if nearly isotropic, will appear less reflective than it actually is due to the gain reduction being applied by the reference BRDF. This should not be a problem as long as the users are aware of the source of the darkening. The amount of darkening in the specular area can actually benefit scene type discrimination.

The implementation of the BRDF gain correction will be beneficial to the meteorological community as a whole. A better understanding of the bidirectional reflectance properties of earth scenes as measured by a visible radiometer on a polar orbiting platform will be obtained.

8.0 References

1. Reflectance Characteristics of Uniform Earth and Cloud Surfaces Derived from Nimbus-7 ERB, V. Ray Taylor and Larry L. Stowe, NOAA - National Earth Satellite Service, Washington, D.C., April 4, 1983.

2. Calculating the Reflectance Map, Berthold, K.P., Horn and Robert W. Sjoberg, Applied Optics, Vol. 18, No. 11, 1 June 1979, pp. 1770-1779.

3. Geometrical Considerations and Nomenclature for Reflectance, NBS Monograph 160, F.E. Nicodemus, J.C. Richmond, J.J. Hsia, I.W. Ginsberg, and T. Limperis, National Bureau of Standards, October 1977.

4. Influence of Sky Radiance Distribution on the Ratio Technique for Estimating Bidirectional Reflectance, J.A. Kirchner and S. Youkhana, and J.A. Smith, Photogrammetric Engineering and Remote Sensing, Vol. 48, No. 6, June 1892, pp. 955-959.

5. Anisotropic Reflectance Characteristics of Natural Earth Surfaces, B. Brennan and W.R. Bandeen, Applied Optics, Vol. 9, No. 2, February 1970.

6. Angular Distribution of Solar Radiation Reflected from Clouds as Determined from TIROS IV Radiometer Measurements, I. Ruff, R. Koefler, S. Fritz, J.S. Winston and P.K. Rao, NESC-38, March 1967, pp 65.

7. Measurements of Clouds Reflectance Properties and the Atmospheric Attenuation of Solar and Infrared Energy, M. Griggs and W.A. Marggraf, Convair Division of General Dynamics, AFCRL-68-0003, December 1967, 156 pages.

8. A Preliminary Report on Bidirectional Reflectance of Stratocumulus Clouds Measured with an Airborne Medium Resolution Radiometer, G.T. Cherrix and B.A. Sparkman, Goddard Space Flight Center, NASA TMX-55659, February 1967.

9. Anisotropic Solar Reflectance Over White Sand, Snow and Stratus Clouds, V.V. Salomonson and W.E. Marlatt, Journal of Applied Meteorology, Volume 7, June 1968, pp. 475-483.

10. The Reflectance and Scattering Of Solar Radiation by the Earth, Fred L. Bartman, University of Michigan, Report 05863-11T, NASA contract No. NASr-54(03), December 1968.

11. Earth Reflectance Patterns Measured by Radiometer on High Altitude Balloon Flights, F.L. Bartman, University of Michigan, College of Engineering, NASA contract No. NASr-54(03), December 1968.

12. Monte Carlo Calculations of Light Scattering from Clouds, Gilbert N. Plass and George W. Kattawar, Applied Optics, Vol. 7, No. 3, March 1968, pp. 415-420.

13. Fast Azimuthally Dependant Model of the Reflection of Solar Radiation by Plane-Parallel Clouds, R. Davies, Applied Optics, Vol. 19, No. 2, 15 Jan 1980, pp. 250-255.

14 Bidirectional Reflectance of a Randomly Rough Surface, T.F. Smith, and R.G. Hering, AIAA Paper No. 71-645, April 1971, Thermophysics Conference.

15. Atmospheric Modeling for Space Measurements of Ground Reflectances Including Bidirectional Properties, D. Tanre, M. Herman, P.Y. Deschamps, and A. de Leffe, Applied Optics, Vol. 18, No. 21, 1 November 1979, pp. 3587-3594.

16. Theory of Off-Specular Reflection from Roughened Surfaces, K.E. Torrance and E.M. Sparrow, Journal of the Optical Society of America, Sept. 1967, Vol. 57, pp. 1105-1114.

17. On Angular Distribution of Radiation Reflected from a Ruffled Sea, H. Arst, Institute of Thermophysics and Electrophysics, USSR, pp. 225-233.

18. Atlas of Reflectance Patterns for Uniform Earth and Cloud Surfaces (NIMBUS-7 ERB--61 Days), V.R. Taylor and L.L. Stowe, NOAA Tech. Report NESDIS 10, July 1984.

19. Navy Tactical Applications Guide, Vol. I, Techniques and Applications of Image Analysis, Robert W. Fett, Naval Environmental Prediction Research Facility, 1977.

20. Space Shuttle Cloud Photographs Assist in Correcting Meteorological Satellite Data, J.W. Snow et al, EOS, Vol. 66, No. 24, 11 June 1985, pp. 489-490.

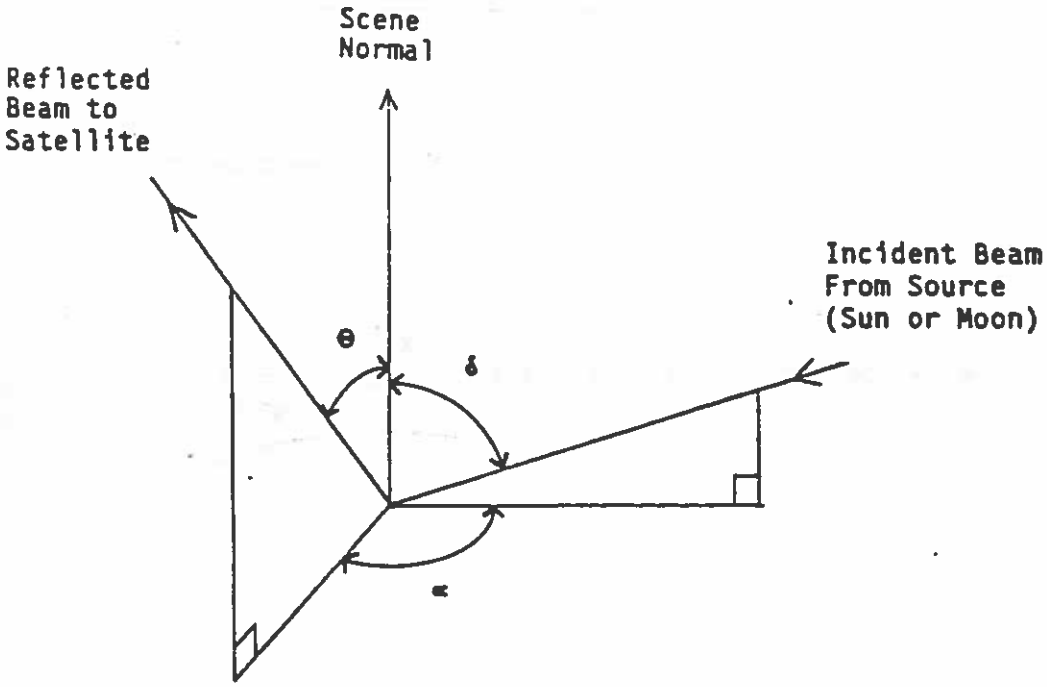

δ = Solar Zenith Angle

θ = Spacecraft Zenith Angle

α = Azimuth

Figure 1 - BRDF Geometry and Angular Definitions

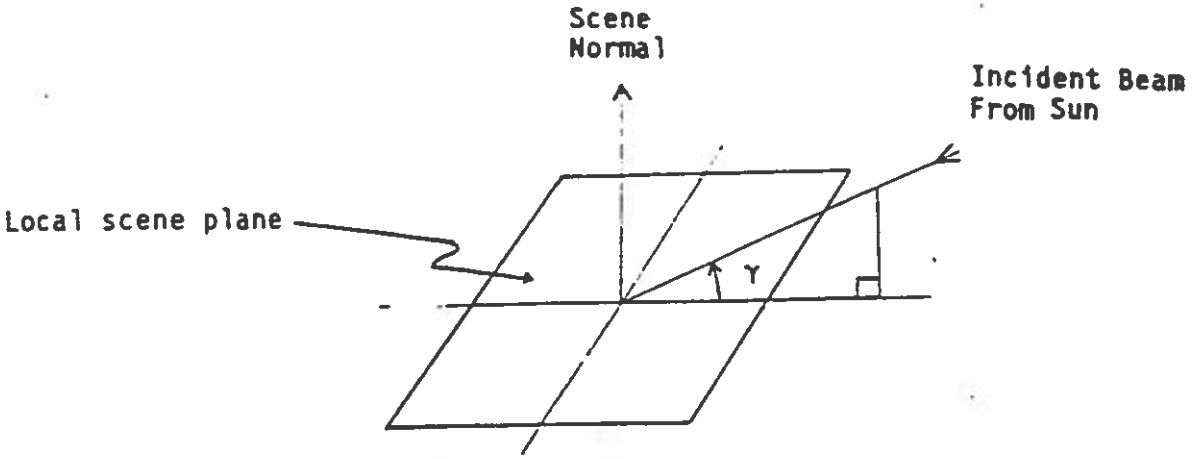

b) Scene Solar Elevation (γ)

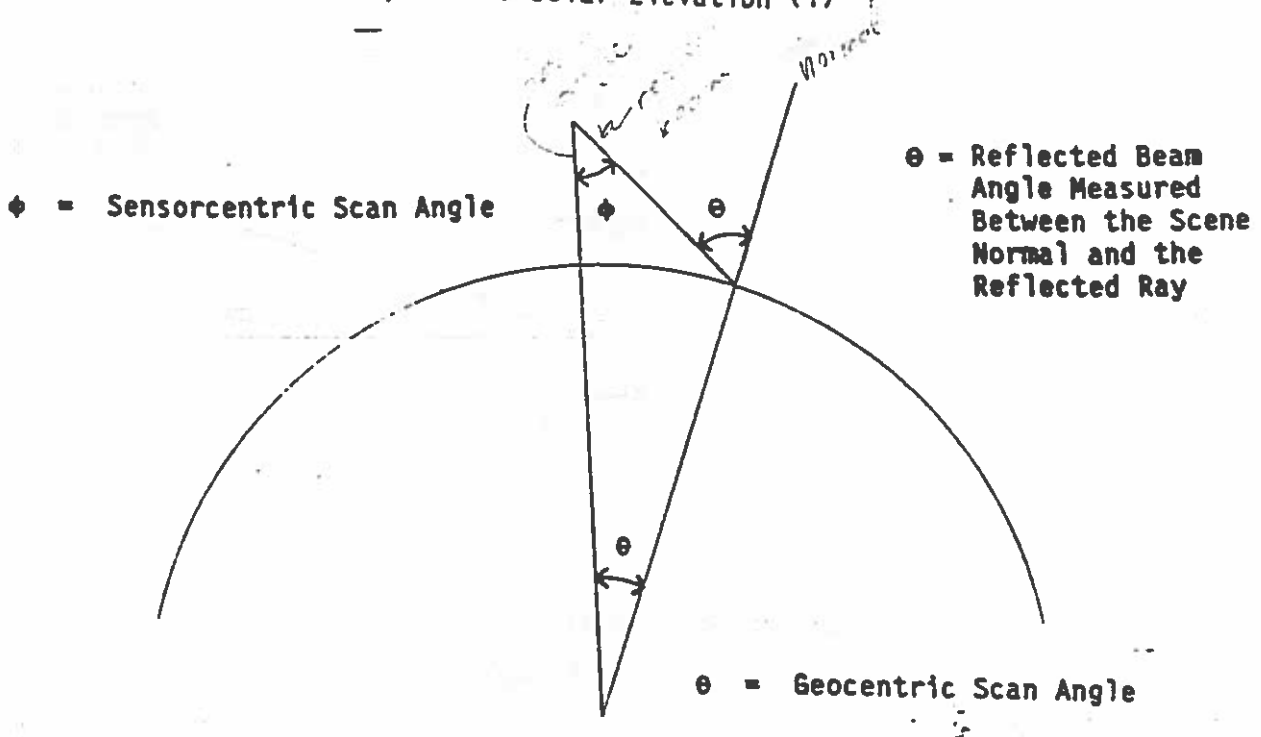

$$\Theta = \phi + \theta$$

a) Scan Angle

Figure 2 - Spacecraft Angular Parameters

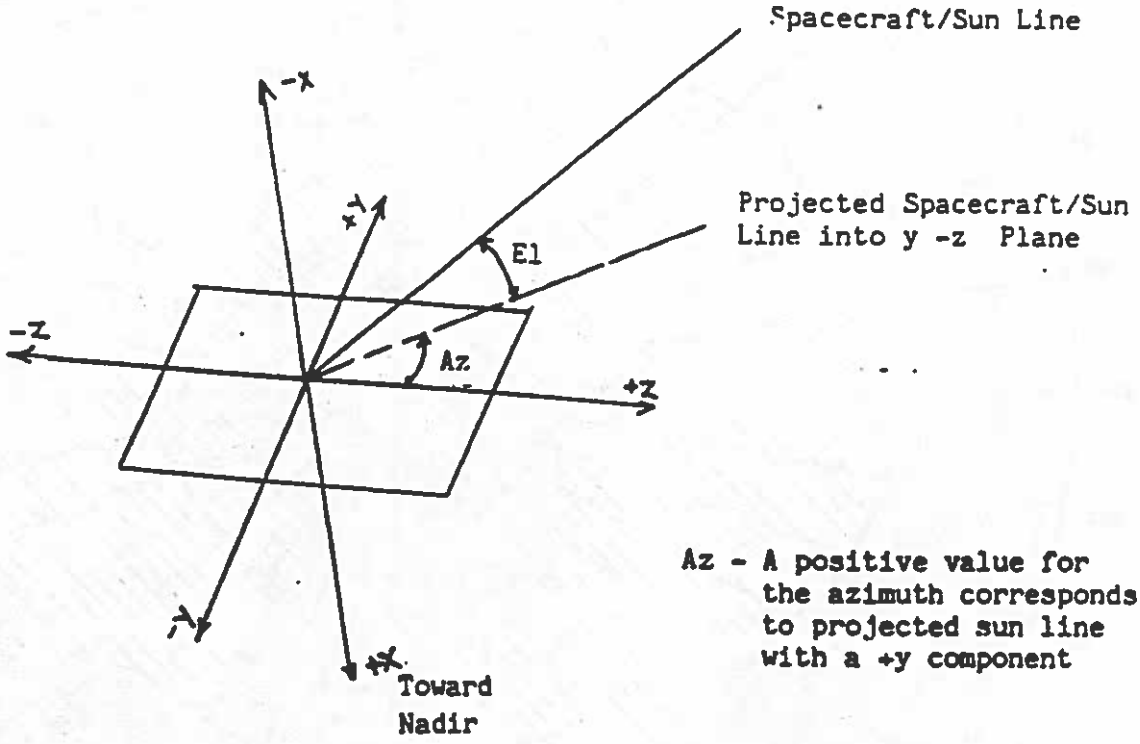

Az - A positive value for the azimuth corresponds to projected sun line with a +y component

z-axis - along scan, +z sunward
y-axis - along track, +y in direction of travel
x-axis - toward nadir, +x toward earth

c) Azimuth and Elevation

Figure 2 - cont.

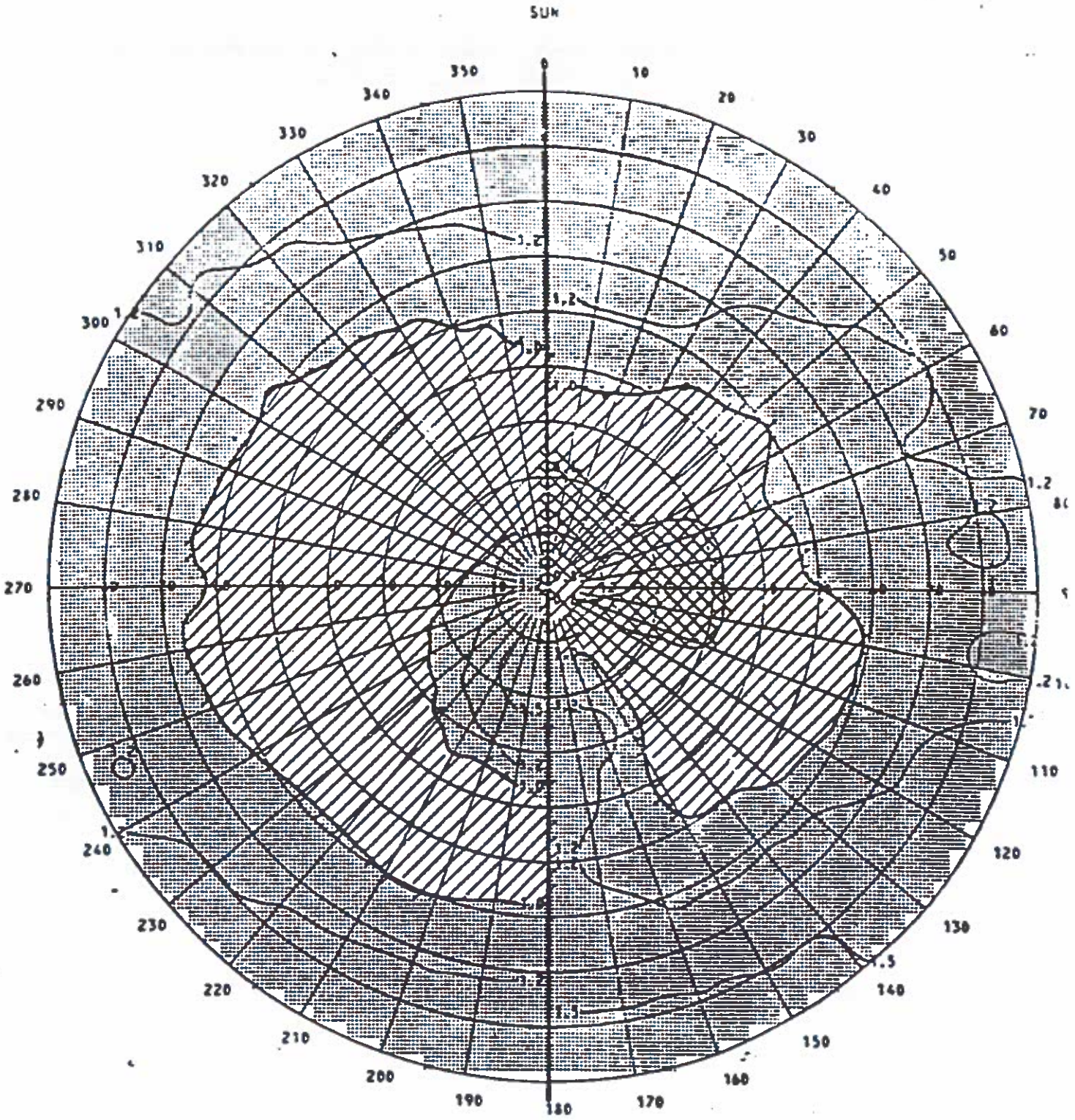

a) θ=0 - 25.8°

b) θ=25.8 - 36.9°

Figure 3 - Nimbus-7 Polar BRDF Plots

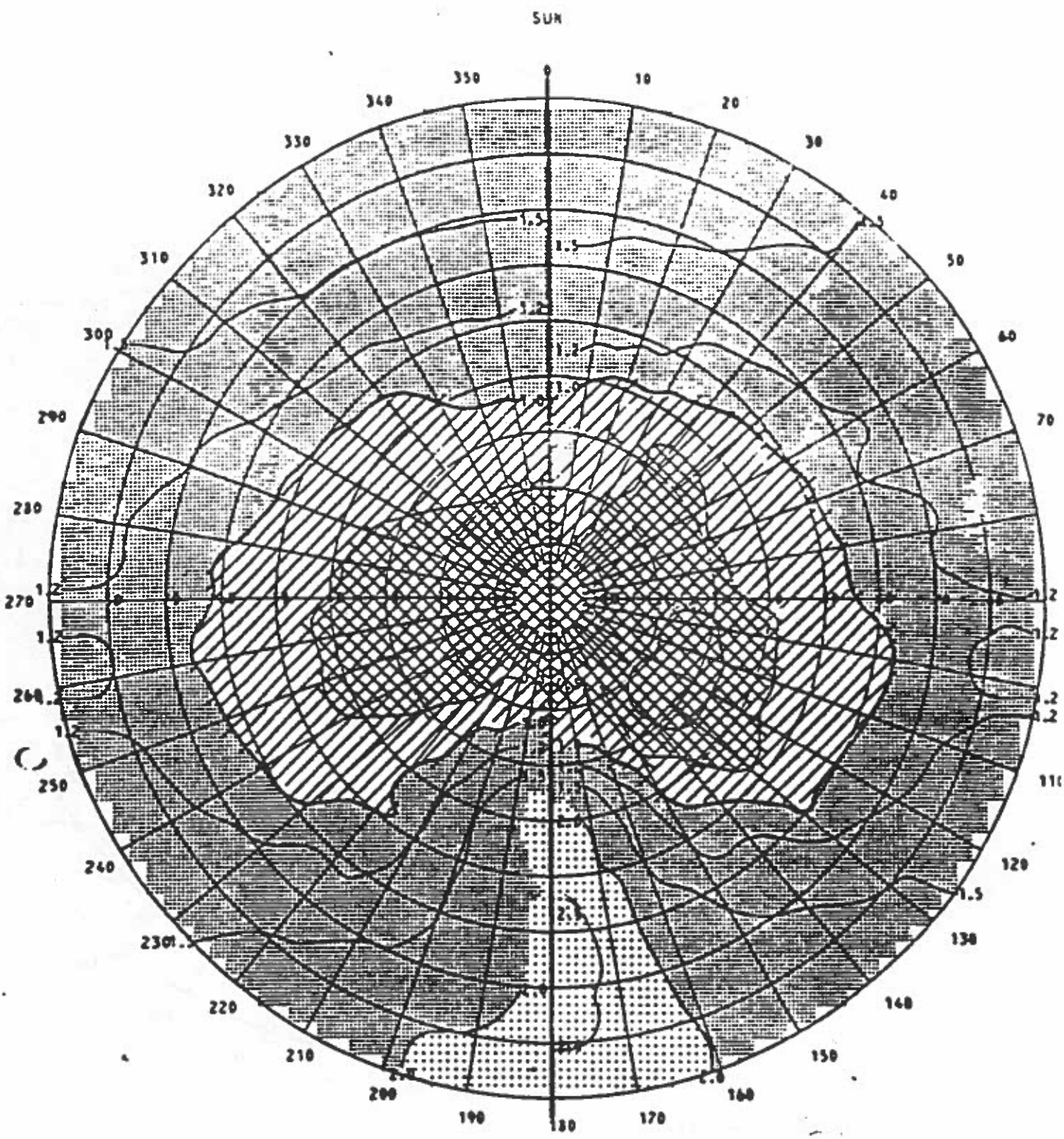

c) δ =45.6 - 53.1°

Figure 3 - cont.

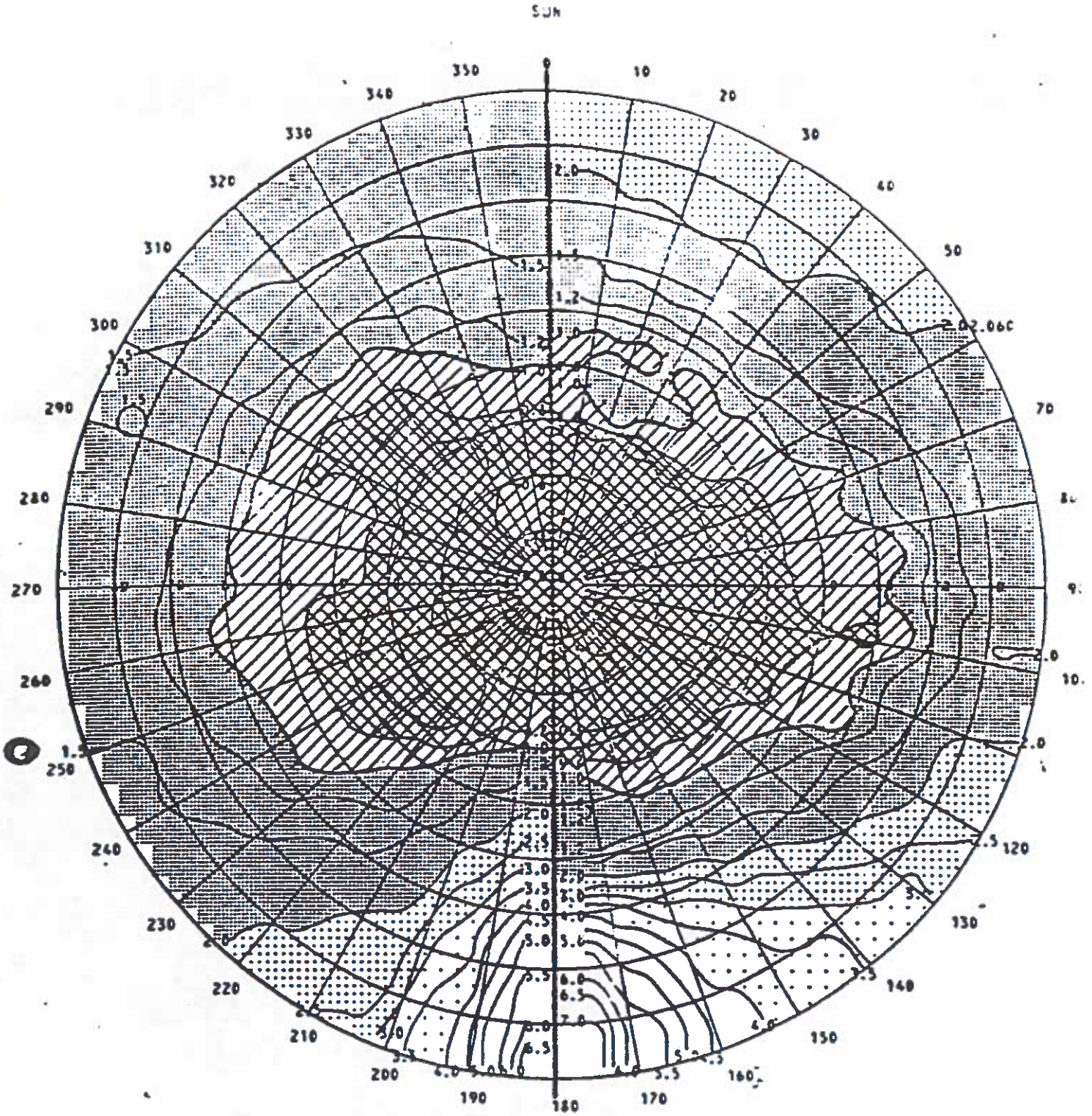

d) δ=60 -66.4°

e) δ=84.3 - 90°

Figure 3 - cont.

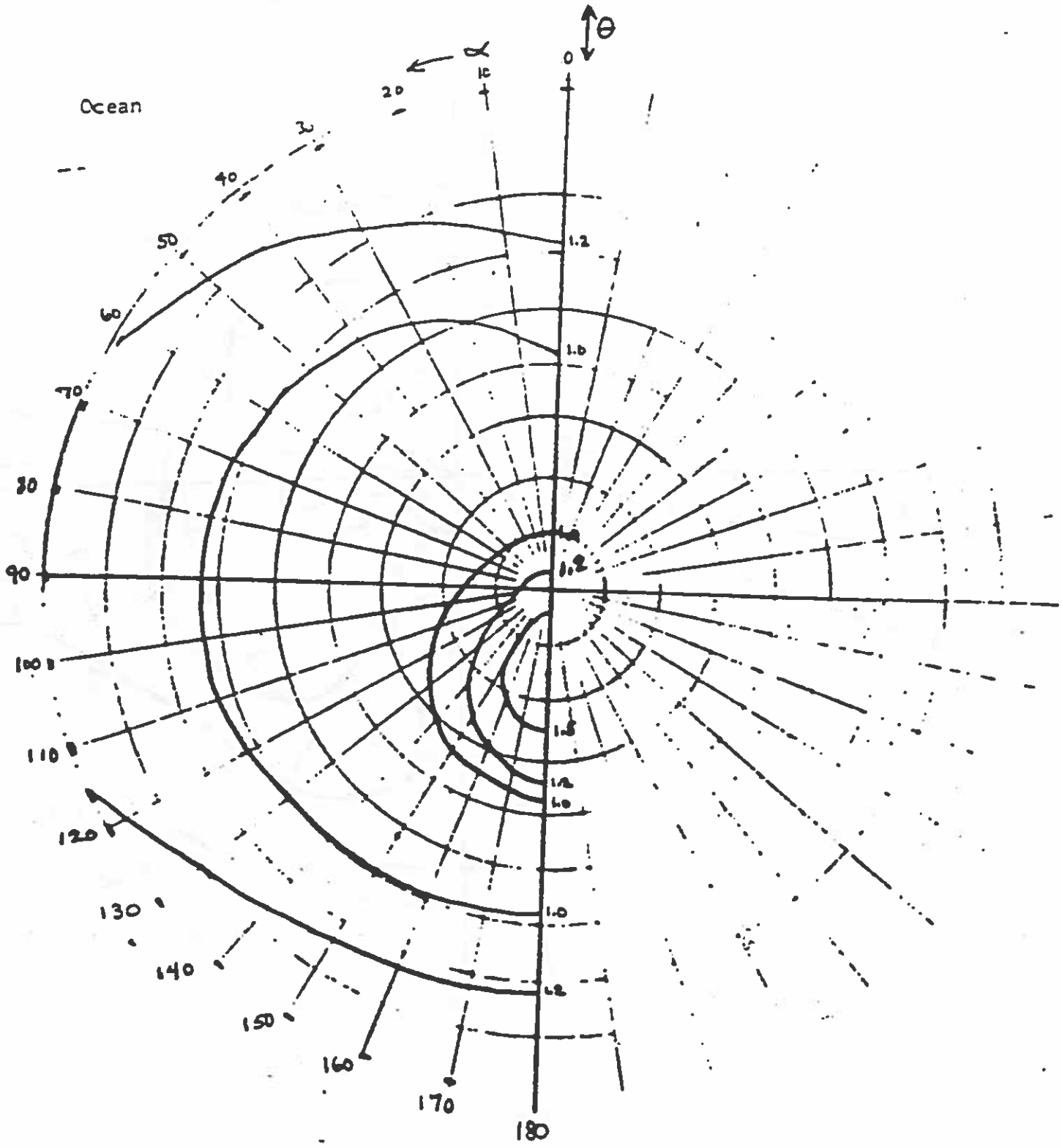

a) $\bar{S}$=0 - 25.8°

Figure 4 - Smoothed Nimbus-7 Polar BRDF Plots

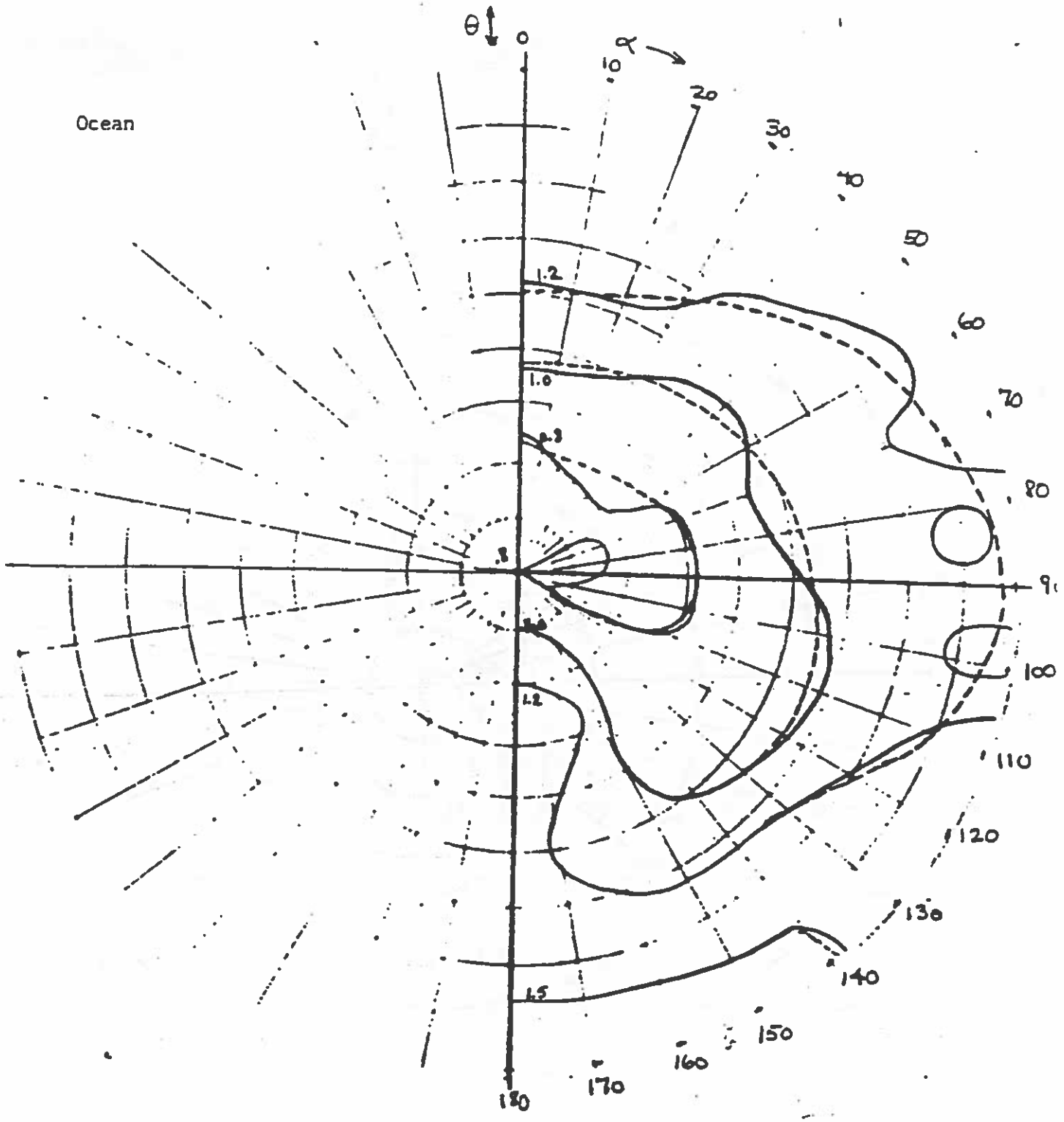

b) δ=25.8 - 36.9°

Figure 4 - cont.

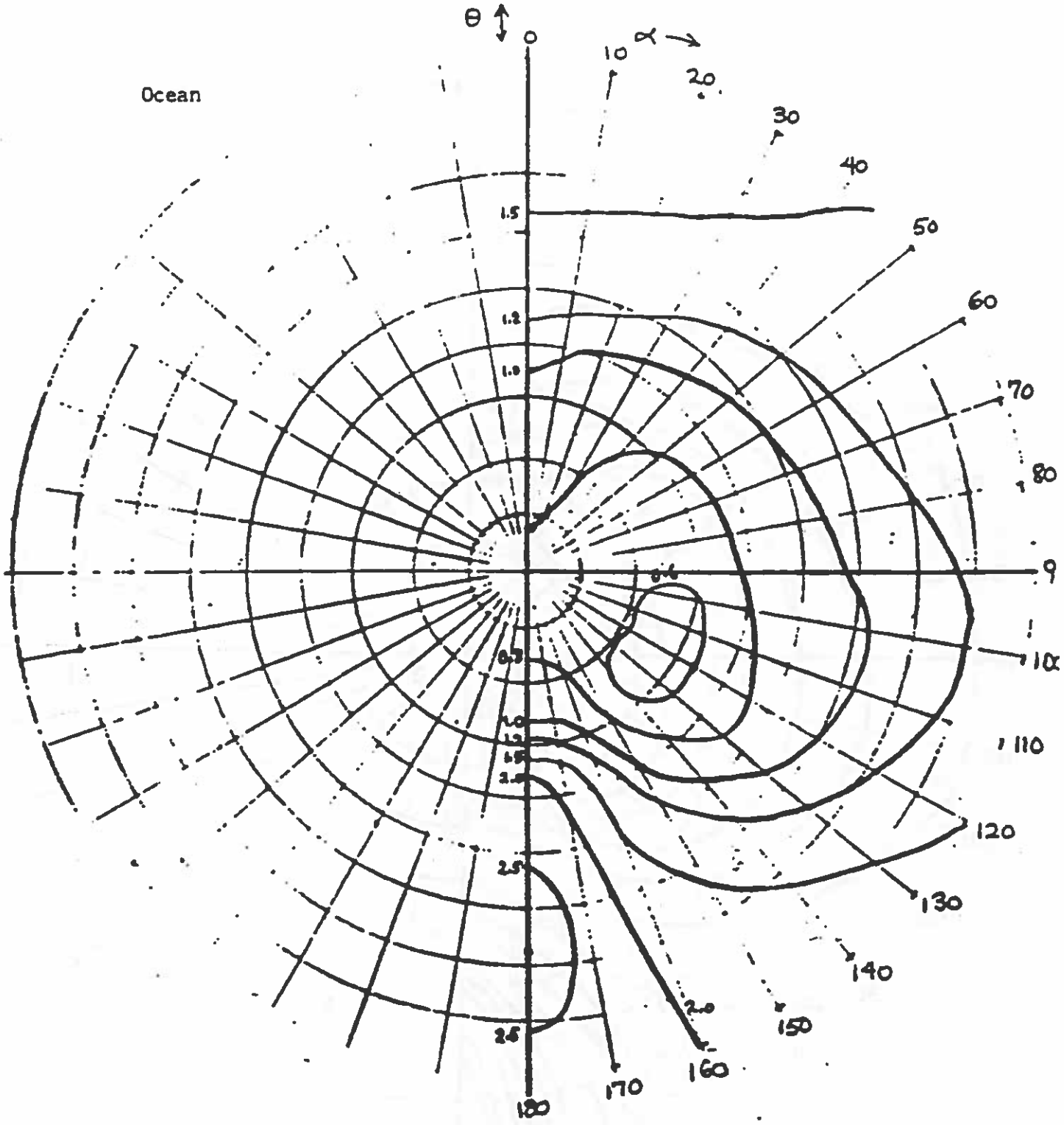

c) $\bar{S}$=45.6 - 53.1°

Figure 4 - cont.

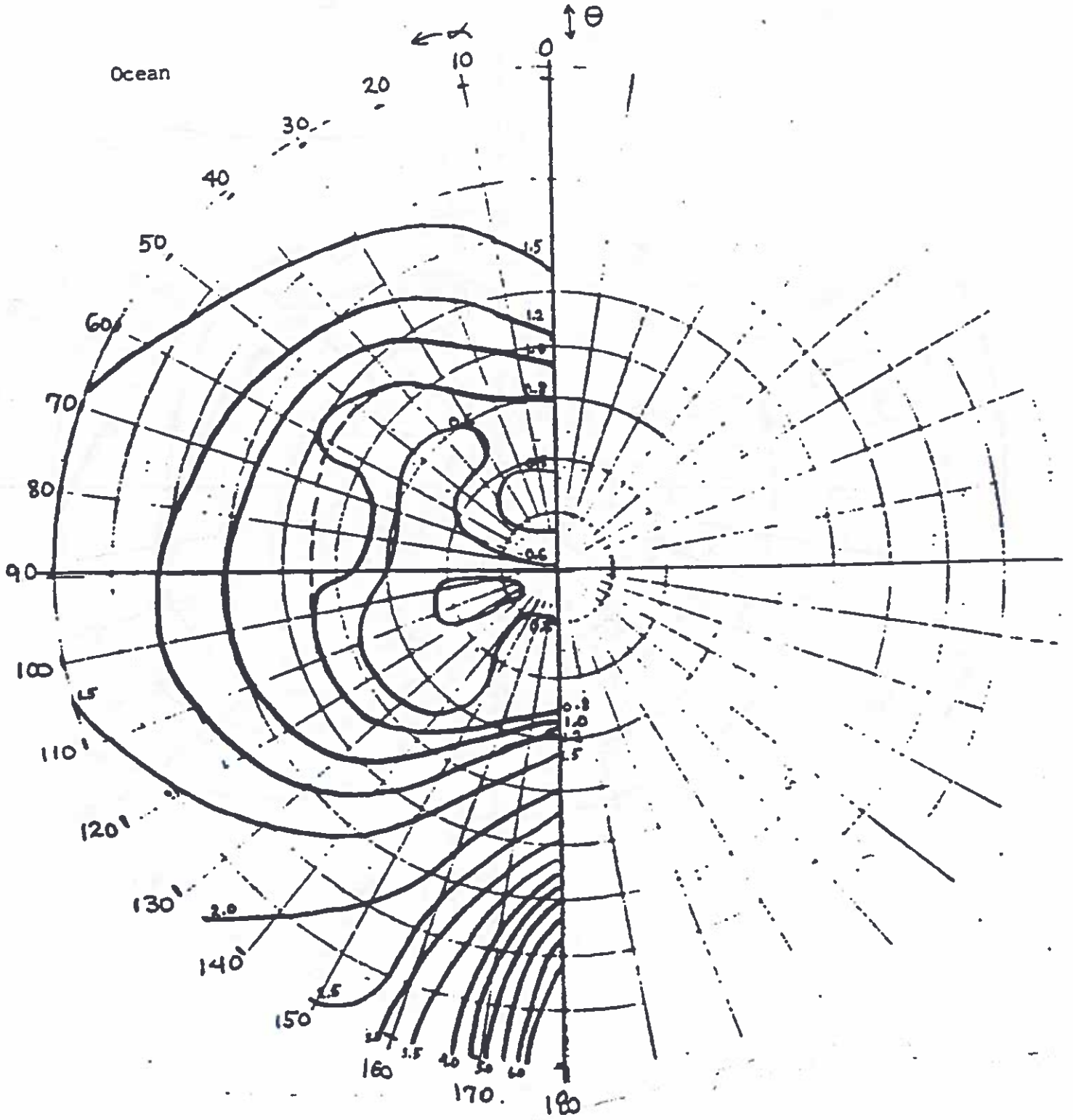

d) $\delta = 60 - 66.4°$

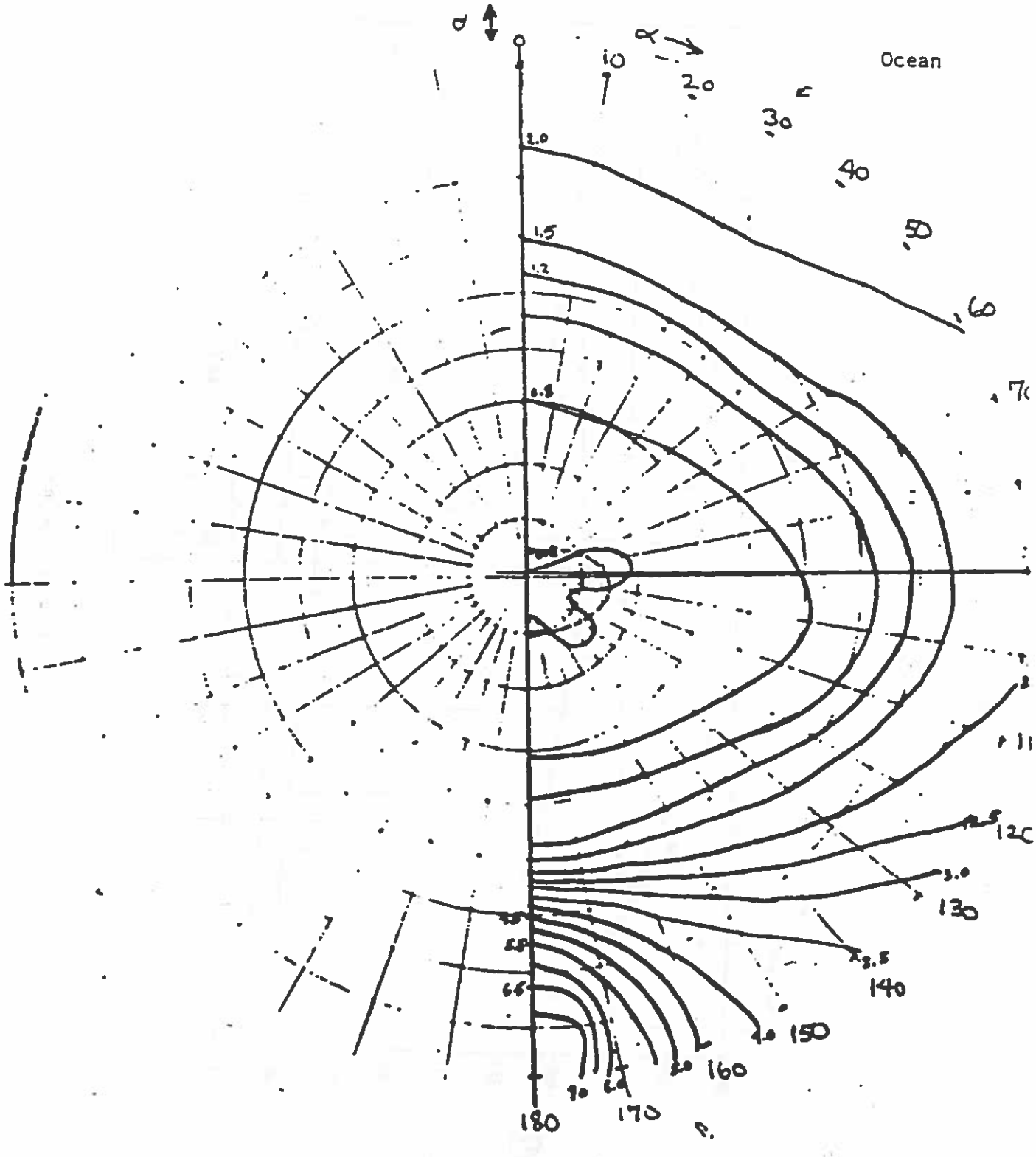

e) δ=84.3 - 90°

Figure 4 - cont..

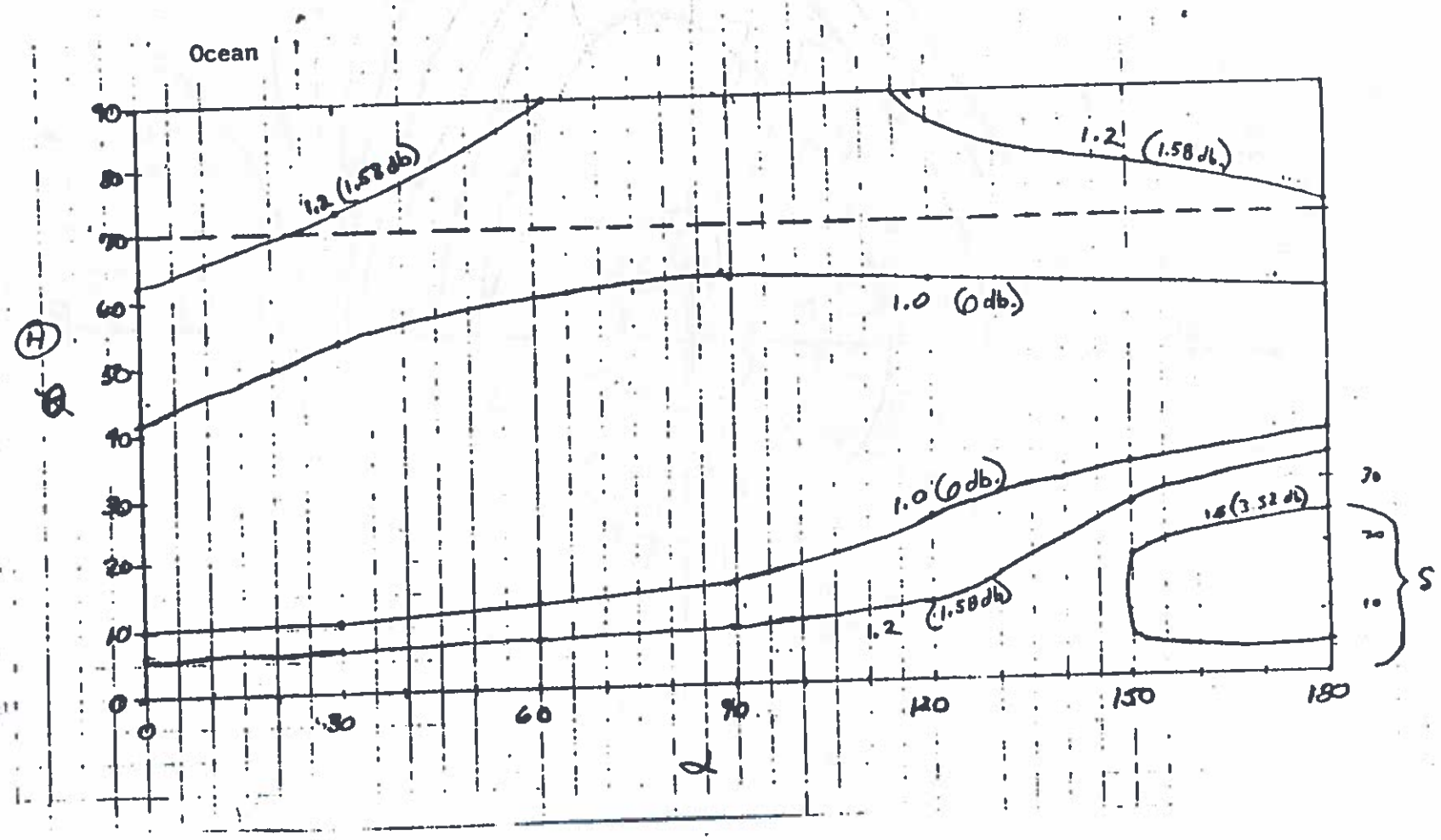

a) $S=0 - 25.8°$

Figure 5 - Smoothed Nimbus-7 Rectilinear BRDF Plots

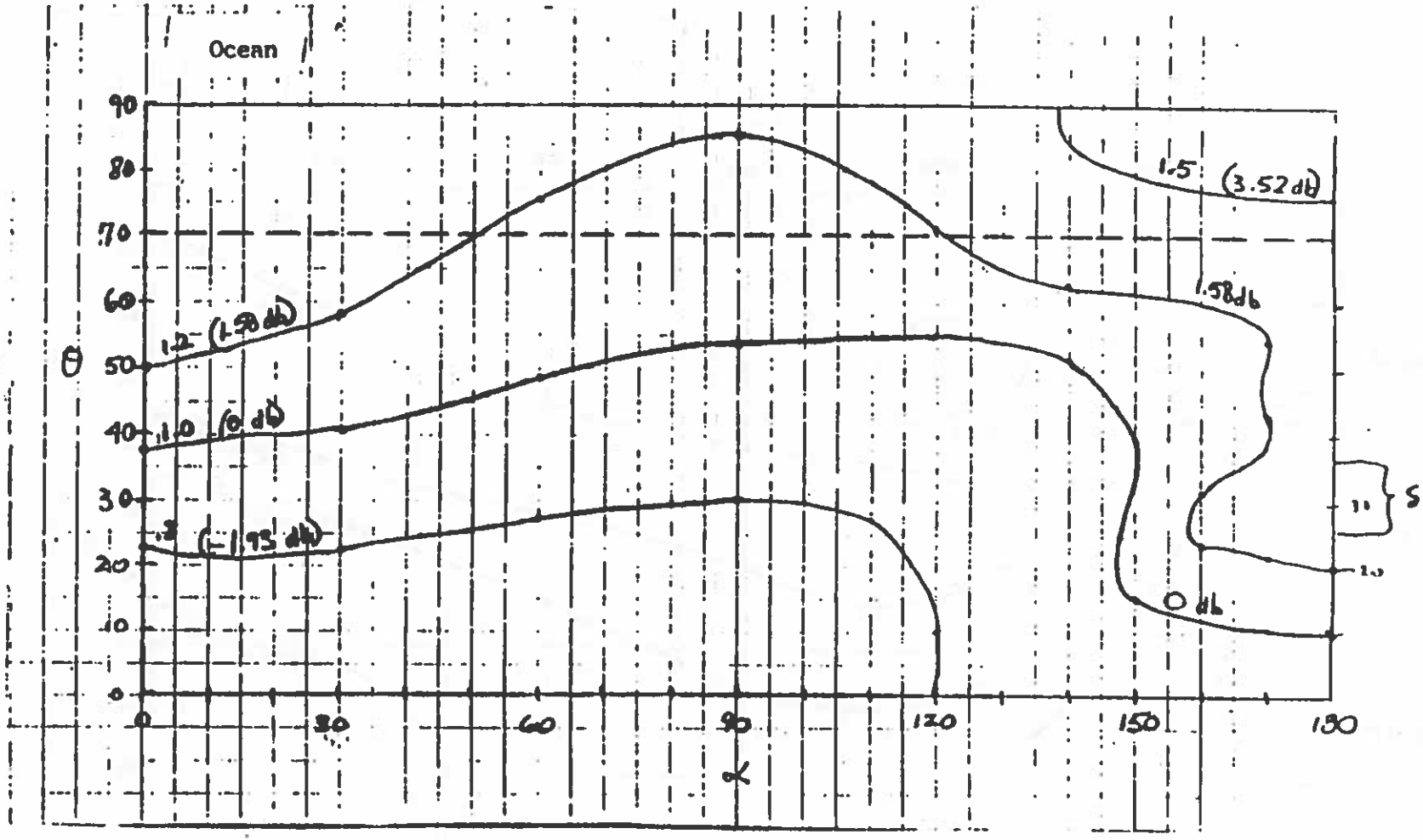

b) S=25.8 - 36.9°

Figure 5 - cont.

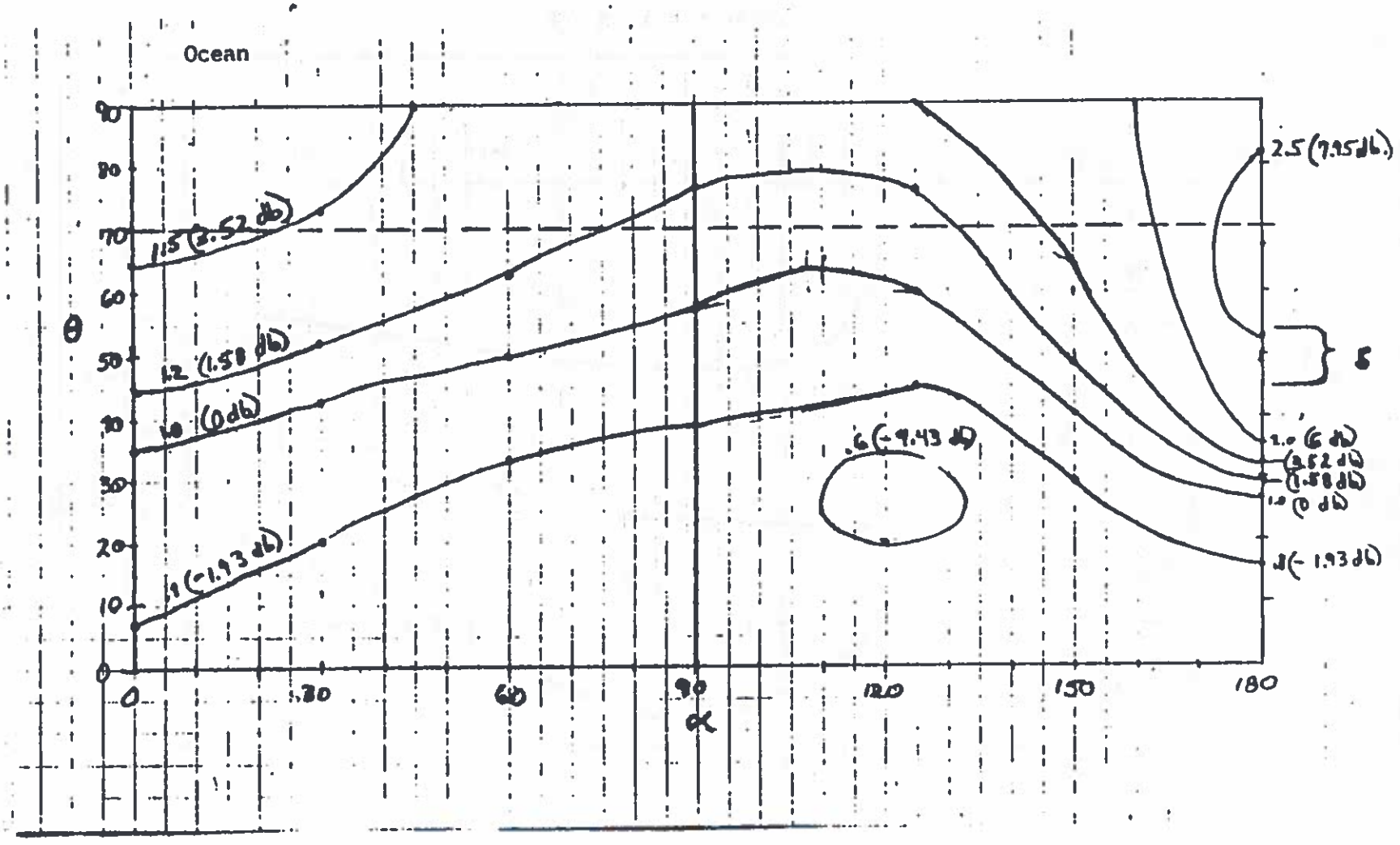

c) S=45.6 - 53.1°

Figure 5 - cont.

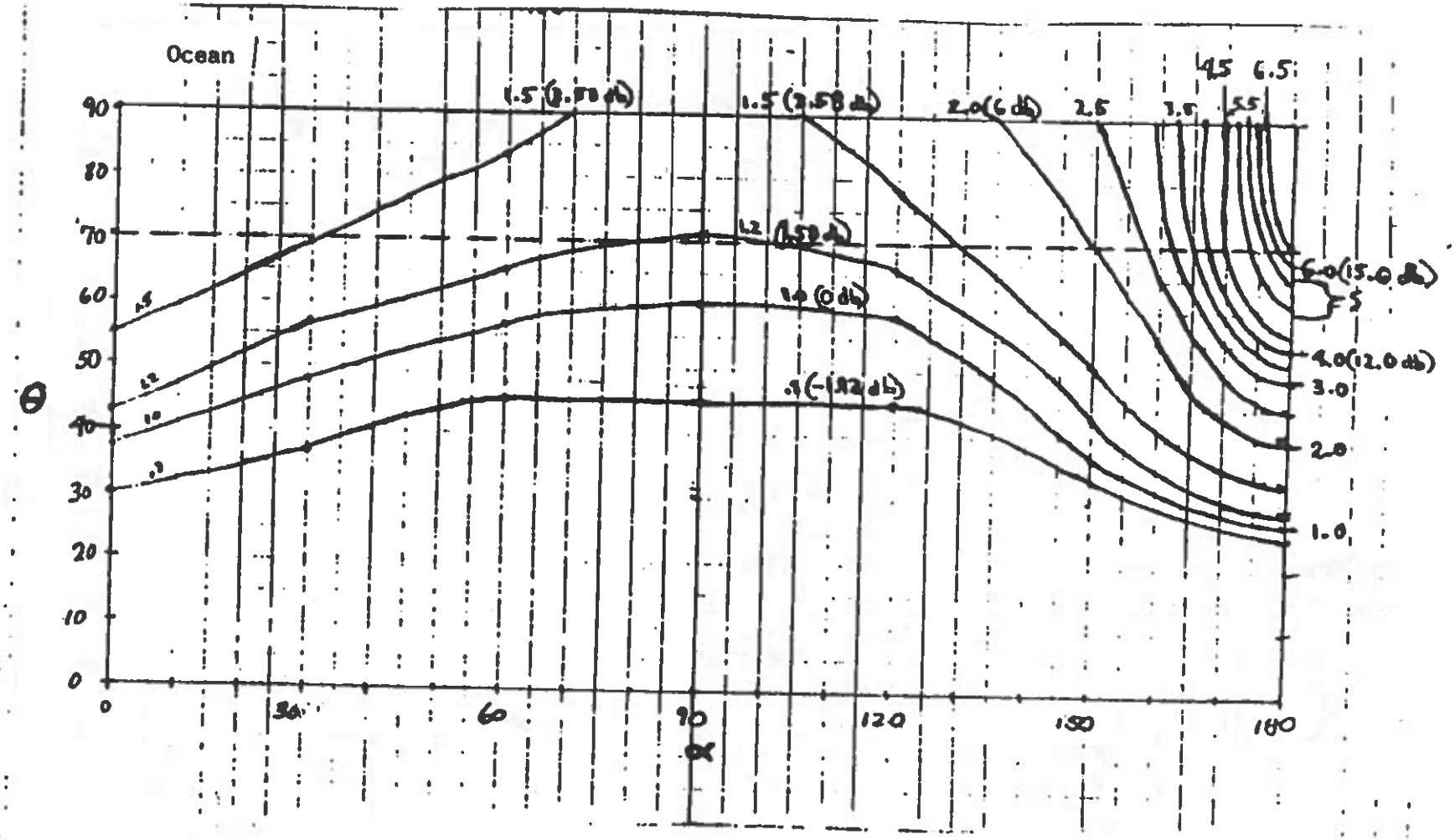

d) S=60 - 66.4°

Figure 5 - cont.

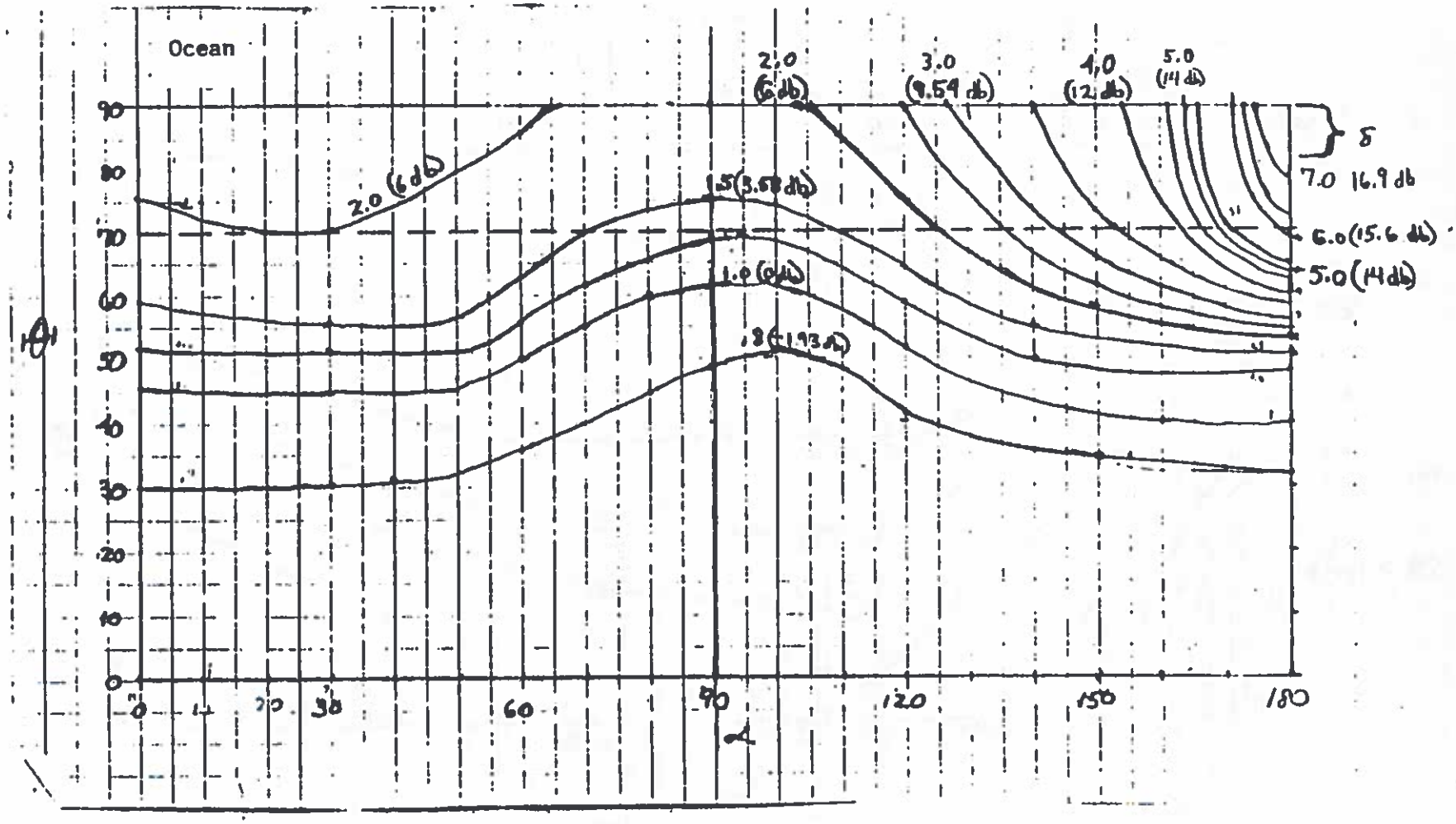

e) δ=84.3 - 90°

Figure 5 - cont.

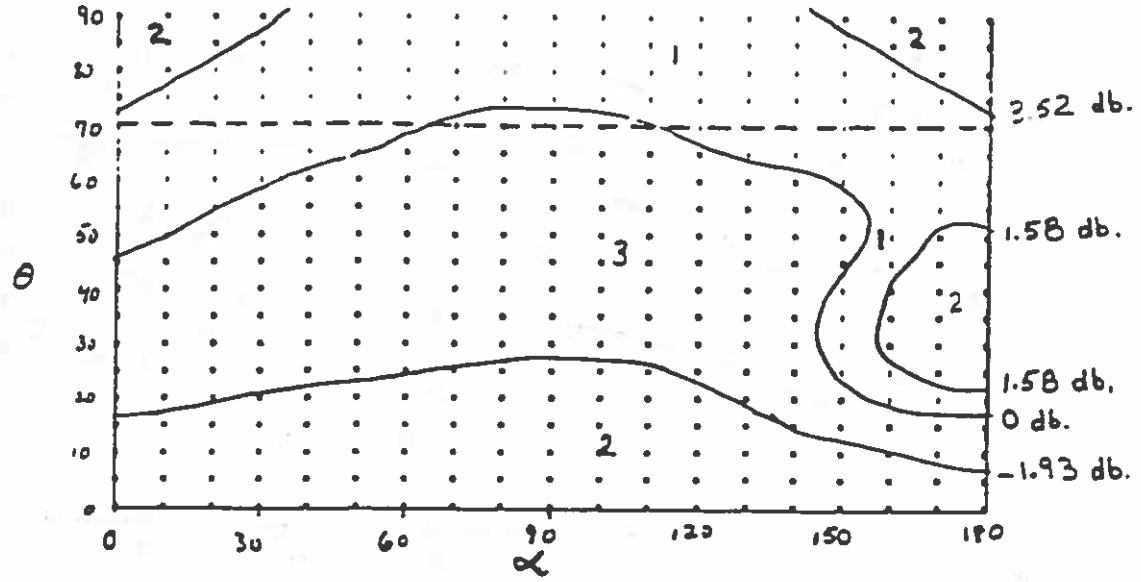

b) $\delta = 31.5°$

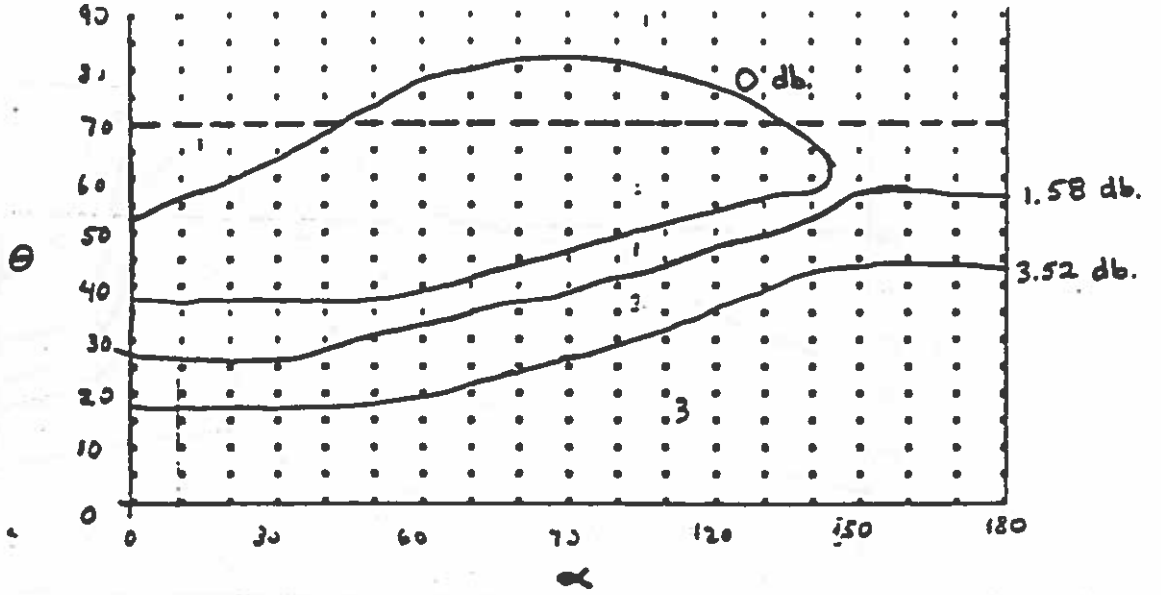

a) $\delta = 13°$

Figure 6 - Computer Generated BRDF Model Plots
Without Sensitivity Correction Factor

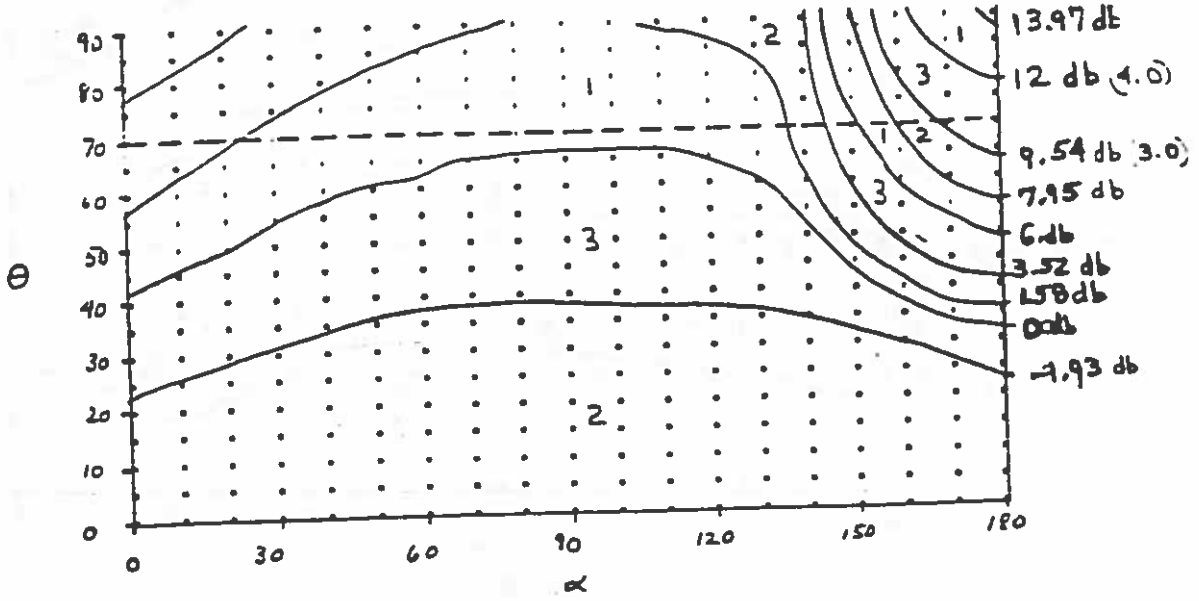

d) $\delta = 63^\circ$

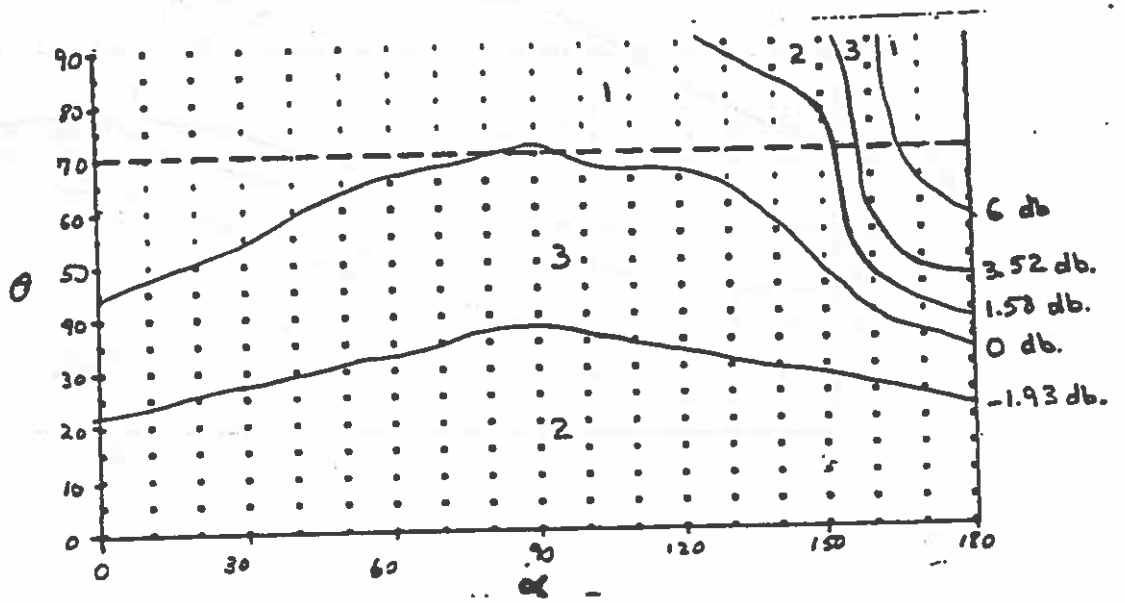

c) $\delta = 49^\circ$

Figure 6 - cont.

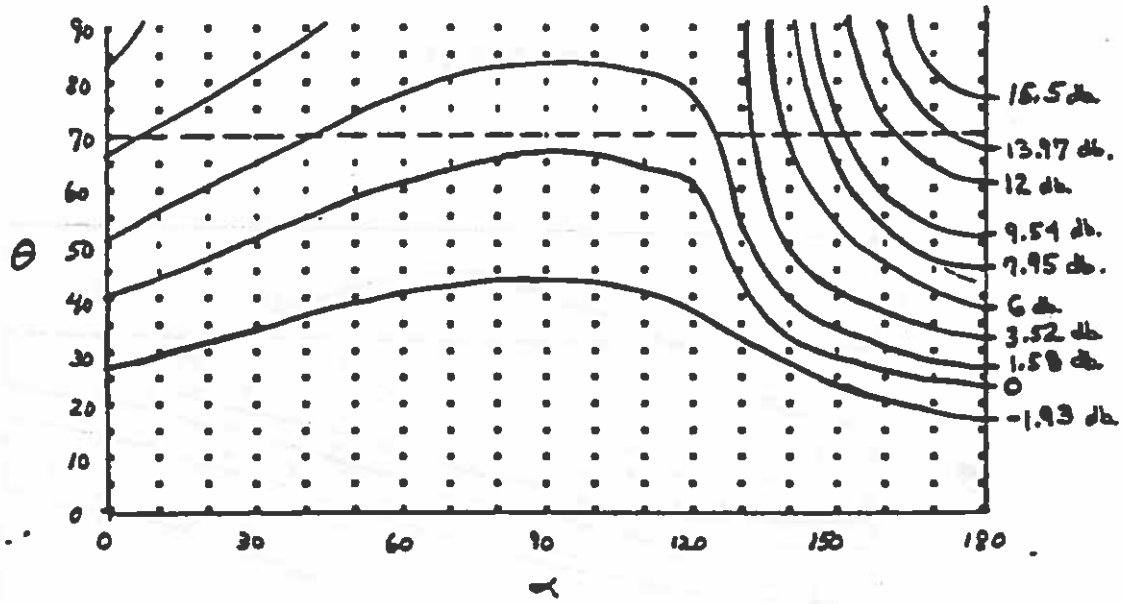

e) $\delta = 87°$

Figure 6 - cont.

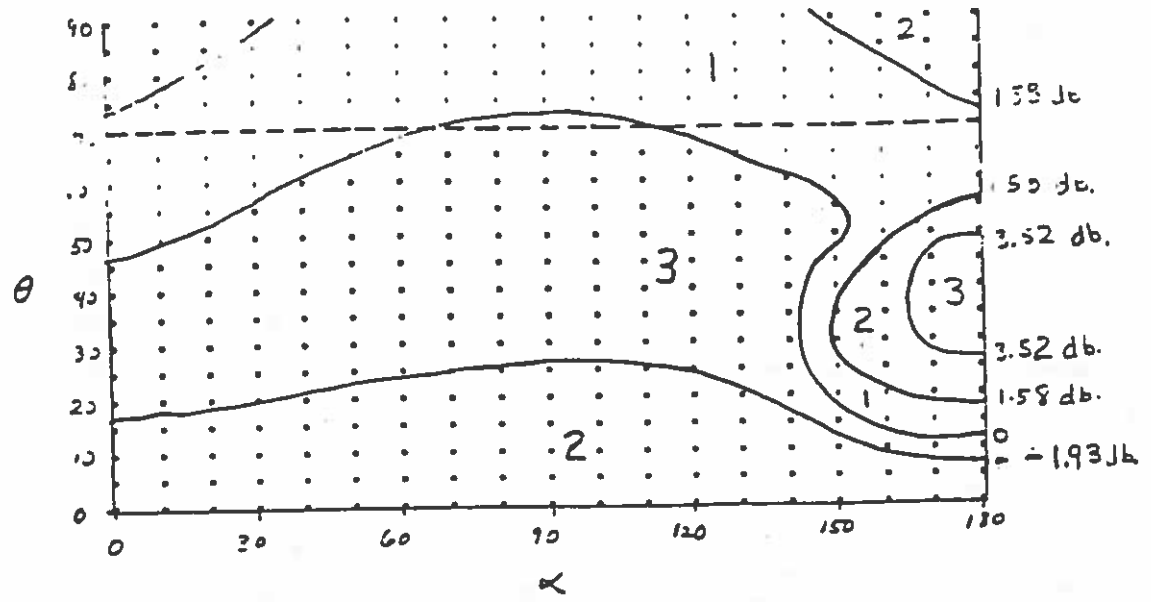

b) δ=31.5°

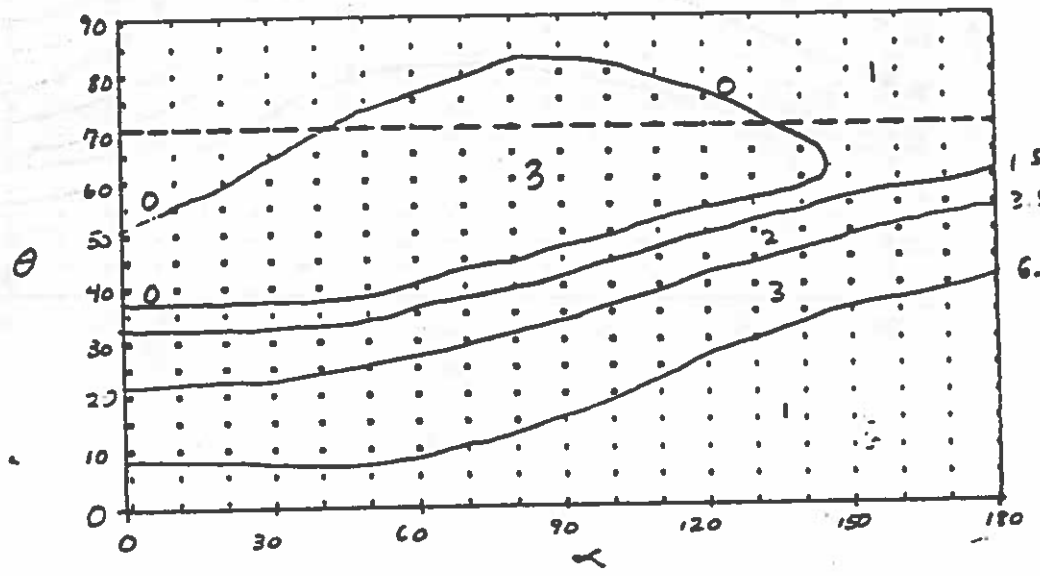

a) δ=13°

Figure 7 - Computer Generated BRDF Reference Model With Sensitivity Correction Factor

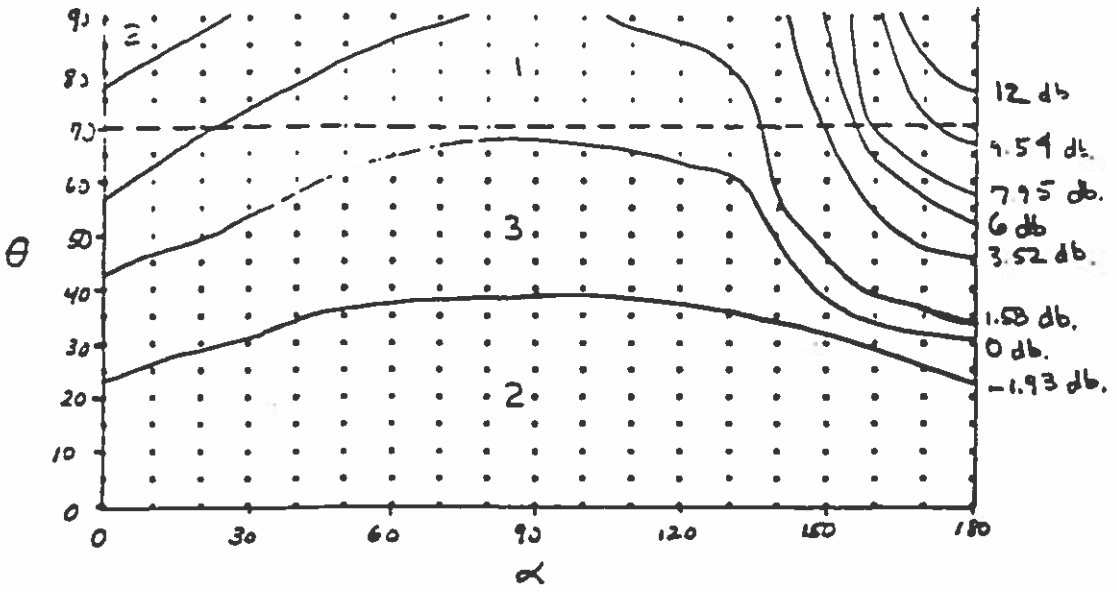

d) $\delta = 63°$

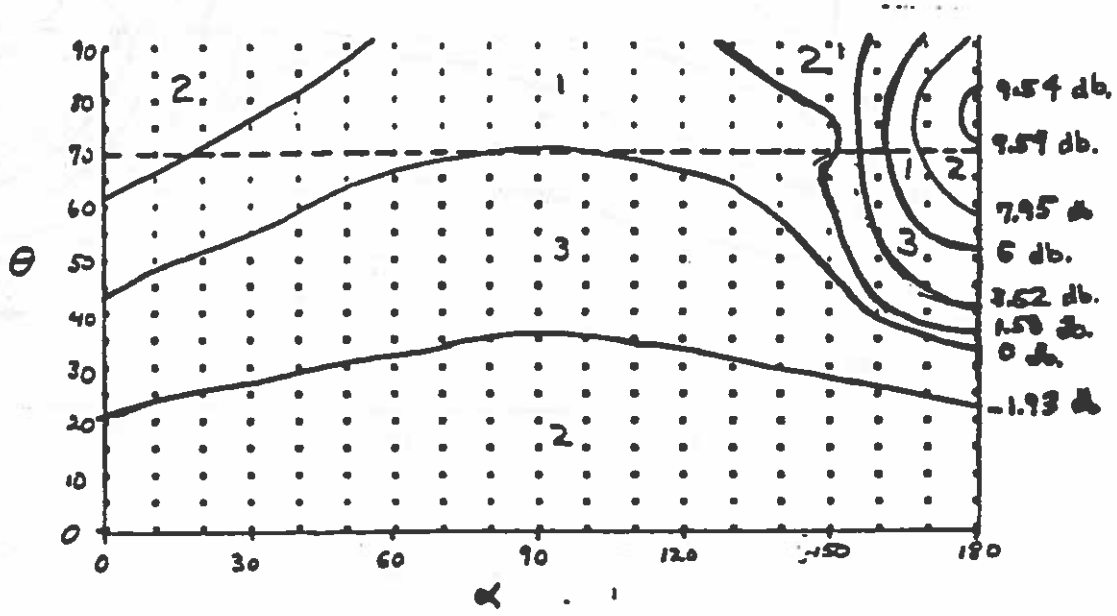

c) $\delta = 49°$

Figure 7 - cont.

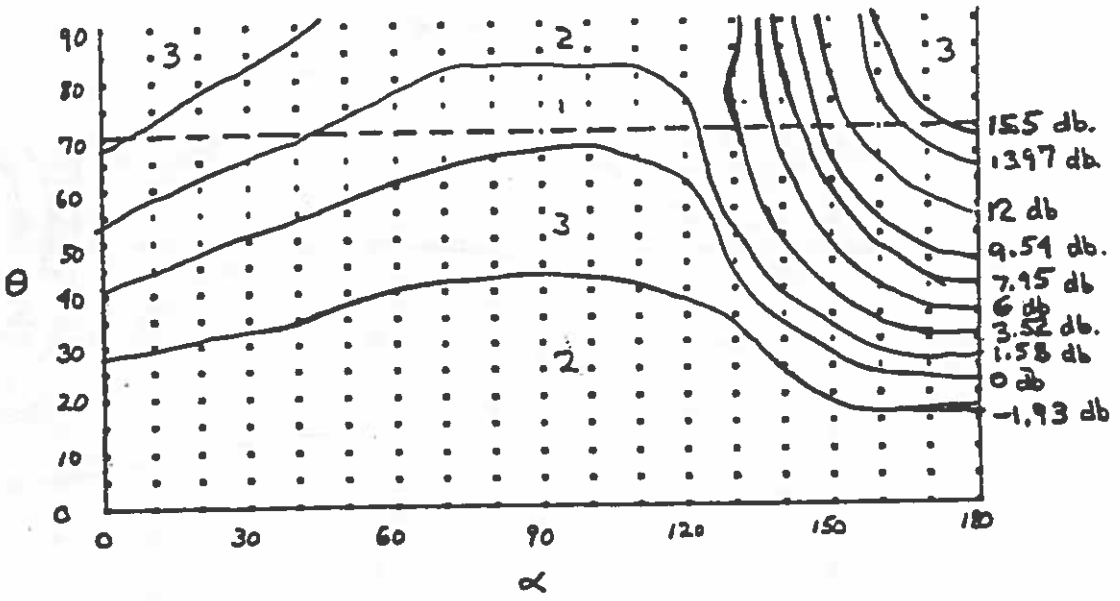

e) $S = 87^{\circ}$

Figure 7 - cont.